

# Preparation and properties of red phosphor CaO: Eu<sup>3+</sup>

Ming Kang · Xiaoming Liao · Yunqing Kang ·  
Jun Liu · Rong Sun · Guangfu Yin ·  
Zhongbing Huang · Yadong Yao

Received: 24 June 2008 / Accepted: 26 January 2009 / Published online: 5 March 2009  
© Springer Science+Business Media, LLC 2009

**Abstract** In this study, the co-precipitation method was adopted to synthesize red phosphor CaO: Eu<sup>3+</sup>. Sodium carbonate was chosen as the precipitator, and sodium dodecylbenzenesulfonate as the surfactant. The structure, morphology, and spectroscopic properties of the samples were characterized by XRD, laser particle size analyzer, SEM, FT-IR, Raman, UV-Vis and PL-PLE spectra, respectively. The results indicated that the Eu<sup>3+</sup> ion inhabited the site of Ca<sup>2+</sup> as the luminescent center, and the crystal structure of cubic CaO remained unchanged. The particle size of the obtained product was 0.5–2 μm with smooth surface. There was a main intense band with a maximum at 250 nm, which was attributed to the charge transfer transition of Eu<sup>3+</sup>-O<sup>2-</sup> and the maximum emission wavelength is 592 nm, corresponding to magnetic dipole transitions <sup>5</sup>D<sub>0</sub> → <sup>7</sup>F<sub>1</sub> of Eu<sup>3+</sup> in the excitation spectrum.

## Introduction

Rare-earth ions as special luminescent center were doped into different hosts, have been widely used, such as

lighting, information display, and optoelectronics technology. Eu<sup>3+</sup> ion is an especially important activator for red phosphors which has been extensively studied for years [1, 2], because the visible emission of Eu<sup>3+</sup> ion in 4f shell is insensitive to the influence of the surroundings due to the shielding effect of 5s, 5p electron [3].

More recently, the alkaline earth oxides as hosts for trivalent europium ions, which substitute alkaline earth ions readily into the lattice, exert further interest in their fundamental properties. Also, because of good luminescent characteristics and chemical stability in vacuum, the oxide-based phosphors attracted extensive attention. It seems to be a good potential choice for the field emission display (FED) red phosphor [4]. The CaO: Eu<sup>3+</sup> is expected to act as one of the most promising red luminescent materials [5]. However, it has been simply synthesized through the traditional high-temperature solid-state method. The product prepared by this method is mostly with either irregular morphology or agglomerate with serious reunion and high hardness, which affects the luminescence efficiency of the phosphors during the later milling.

As we know different material preparation methods have some important effects on material microstructure and physical properties. The chemical solution technique has the unique advantages over the high-temperature solid-state method such as high purity, fine particles, and homogeneity in atomic size level. Among the chemical solution technique, the co-precipitation technique has been widely adopted because the particle size of product could be easily controlled and the mono-dispersed red phosphor powders are readily prepared [6–8].

In this study, the red phosphor CaO: Eu<sup>3+</sup> was prepared for the first time by the modified solid-state reaction method. The precursor was synthesized with the precipitation agent of sodium carbonate and the template of

---

Ming Kang and Xiaoming Liao contributed equally to this work.

M. Kang · X. Liao · Y. Kang · G. Yin (✉) · Z. Huang · Y. Yao  
College of Materials Science and Engineering,  
Sichuan University, Chengdu 610064, Sichuan, China  
e-mail: nic0700@scu.edu.cn

M. Kang  
e-mail: mingkang20082008@hotmail.com

M. Kang · J. Liu · R. Sun  
Southwest University of Science and Technology,  
Mianyang 621010, China

sodium dodecylbenzenesulfonate. The sample was characterized with XRD, laser particle size analyzer, SEM, FT-IR, Raman, UV–Vis, photoluminescence and photoluminescence excitation spectra.

## Experimental

### Preparation

The red phosphor CaO: Eu<sup>3+</sup> was prepared from Ca(NO<sub>3</sub>)<sub>2</sub>·4H<sub>2</sub>O, Eu<sub>2</sub>O<sub>3</sub>, Na<sub>2</sub>CO<sub>3</sub> and ammonia through co-precipitation. The corresponding reaction equation is shown in Scheme 1.

Firstly, Eu<sub>2</sub>O<sub>3</sub> was dissolved in dilute HNO<sub>3</sub> to form Eu(NO<sub>3</sub>)<sub>3</sub> solution. Then appropriate amounts of Ca(NO<sub>3</sub>)<sub>2</sub>·4H<sub>2</sub>O were dissolved in distilled water and mixed with aqueous solution of europium, and stirred by magnetic stirrer at 40 °C. The pH value was set at about 5–6 by dilute ammonia. Secondly, appropriate volume of Na<sub>2</sub>CO<sub>3</sub> and sodium dodecylbenzenesulfonate solution was put into the solution of Ca(NO<sub>3</sub>)<sub>2</sub> and Eu(NO<sub>3</sub>)<sub>3</sub> at a certain speed. Then the obtained deposition was aged in 40 °C water for 1.5 h. The precursor was gained through the process of filtering, washing with distilled water and ethanol and drying at 80 °C. In the last step, precursor was calcined at 1100 °C for 2 h in air to obtain the oxide phosphor CaO: Eu<sup>3+</sup>. The doping concentration of Eu<sup>3+</sup> is 1 mol% relative to CaO host lattice.

### Characterization

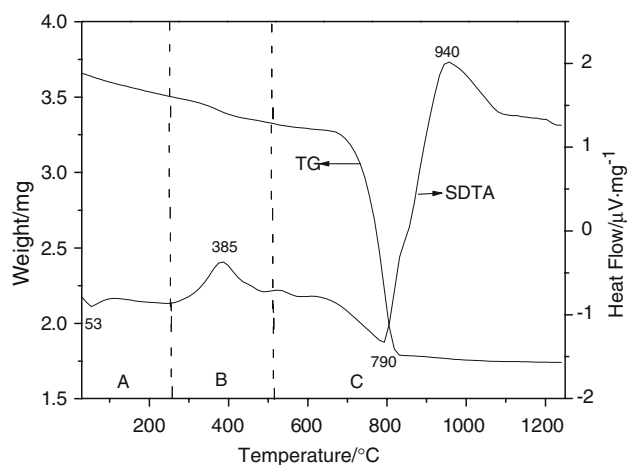
Synchronization of differential thermal analysis (SDTA) and thermogravimetric (TG) analysis of the precursor were carried out with TG/SDTA851<sup>c</sup> analyzer (METTLER-TOLEDO Co., Switzerland) at the heating rate of 10 °C/min in air. The X-ray diffraction (XRD) was performed using a Japan Rigaku D/max-III B diffractometer operating with Cu K $\alpha$  radiation ( $\lambda = 0.15406$  nm) at 35 kV/60 mA. A step size of 0.02°/2 $\theta$  was used with a scan speed of 8°/min. The shape and size of sample were examined by the scanning electron microscope (SEM) utilizing a Hitachi TM-1000 scanning electron microscope and Mastersizer 2000, respectively. The Fourier transform infrared (FT-IR) spectra were recorded in the 225–4000 cm<sup>-1</sup> region using KBr pellets on a Nicolet-5700 infrared spectrometer. Micro-Raman measurement was taken with an InVia Renishaw Raman Microscope System equipped with He–Ne laser at 514.5 nm as excitation source. Diffuse reflectance spectra were taken on UV-3150 spectrophotometer (Japan, Shimadzu, Co.). The luminescence properties of the phosphors

were performed by using a Hitachi F-4500 fluorescence spectrometer with a 150 W-xenon lamp under a working voltage of 400 V. Both the excitation and emission slits were set at 2.5 nm. All the measurements were performed at room temperature.

## Results and discussion

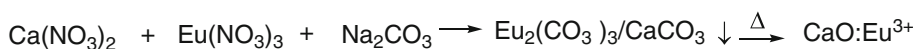
### Thermal behavior analysis of precursor

Typical TG-SDTA curves of the obtained precursor have been given in Fig. 1. Three steps associated with the weight loss can be observed. The first temperature interval step (A) and the weight loss were 30–250 °C and 4.11%, respectively; this weight loss is assigned to the release of residual water adsorbed at the power surface. This water evaporation showed a weak endothermic peak around 53 °C in the SDTA curve. (B) In this stage from 250 to 520 °C, the weight loss was around 4.23%. One exothermic peak was shown in the SDTA curve at 385 °C, which contributed to the sodium dodecylbenzenesulfonate combustion, because there were black impurities in the sample when the firing temperature was 400 °C. (C) In this stage (600–1100 °C and weight loss, 44.05%), the endothermic peak at 790 °C was attributed to decomposition of the basic carbonate and CO<sub>2</sub> and H<sub>2</sub>O released. The next exothermic peak was at 940 °C, corresponding to the crystallization from the amorphous CaO into the crystalline CaO structure.



**Fig. 1** TG-SDTA curves of precursor

**Scheme 1** Preparation of the red phosphor CaO: Eu<sup>3+</sup>



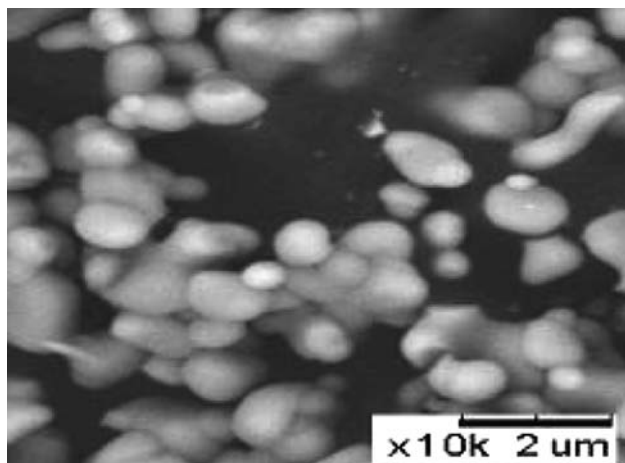


**Fig. 2** SEM micrograph of CaO: Eu<sup>3+</sup> phosphor

#### SEM micrograph and particle size analysis of sample

Crystallinity, particle size, and surface roughness of the phosphor have strong effects on the photoluminescence. Figure 2 exhibits surface morphology of CaO: Eu<sup>3+</sup> particles. It is clear from SEM images that the morphology of the sample was very smooth and interlinked in ellipse. The sample had a mean size of 0.5–2 μm and a very narrow distribution, as evident from the size distribution shown in Fig. 3. This was favorable for the sample. The smooth surface of phosphor can reduce the non-radiation and scattering, thus beneficial to the luminescence efficiency in application [9]. The dense packed small particles can prevent the phosphors from aging.

#### XRD patterns and UV–Vis diffuse reflection spectrum analysis of sample

XRD was used to examine the crystal structure and phase purity of the products, and the typical XRD patterns of the pure CaO and Eu<sup>3+</sup> doped CaO sample are shown in Fig. 4. All the diffraction peaks are assigned to face-centered cubic

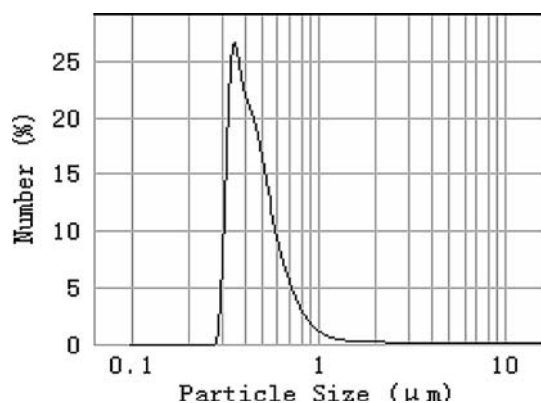


**Fig. 3** Particle size distribution of CaO: Eu<sup>3+</sup> phosphor

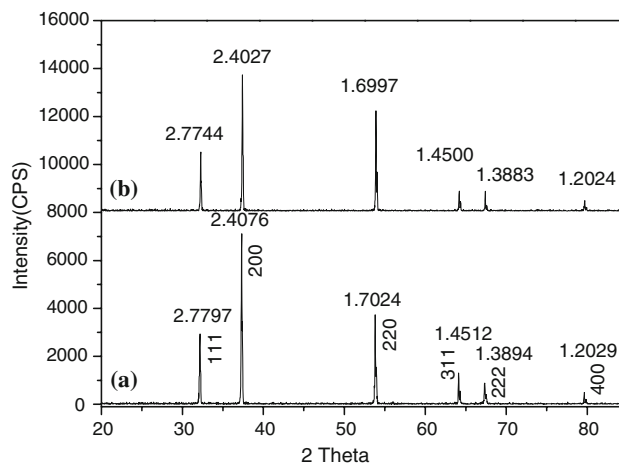


**Fig. 4** XRD patterns of pure CaO (a) and sample CaO: Eu<sup>3+</sup> (b)

crystalline phase of calcium oxide (no. JCPDS 37-1497) with space group  $Fm\bar{3}m$  and no any other impurity phase can be detected, indicating that the doped Eu<sup>3+</sup> ions were occupied the Ca<sup>2+</sup> sites. As the ionic radius of Eu<sup>3+</sup> (0.95 nm, coordination number = 6) is only slightly larger than that of Ca<sup>2+</sup> (0.99 nm, coordination number = 6), Eu<sup>3+</sup> ion is likely to substitute for Ca<sup>2+</sup> ion and acts as the luminescence center [10].

The different is that all three-peak value of  $d$  and cell parameter in XRD pattern of sample ( $d = 2.7797, 2.4076, 1.7024, a = 4.8076$ ) compared to pure CaO ( $d = 2.7744, 2.4027, 1.6997, a = 4.8134$ ) that are somewhat decreased. The reason is that when Ca<sup>2+</sup> ion was substituted by Eu<sup>3+</sup> ion, crystal lattice will have a slight deformation, owing to Eu<sup>3+</sup> ion is smaller than Ca<sup>2+</sup> ion, which leads to the decrease of  $d$  values and cell parameter ( $a$ ).

UV diffuse reflectance and excitation spectrum are carried out to evaluate the crystallization degree and potential optical properties of sample. The UV diffuse

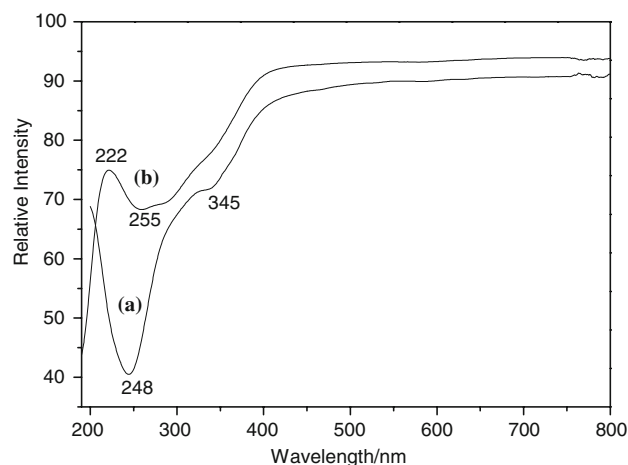


**Fig. 5** Diffuse reflection spectra of Eu<sup>3+</sup>-doped (a) and undoped CaO (b)

reflectance spectra of CaO and CaO: Eu<sup>3+</sup> is shown in Fig. 5. As shown in Fig. 5b, undoped CaO shows one drop in reflection in the UV range around 400 nm with an estimated band gap of about 255 nm, corresponding to absorption of the undoped CaO host lattice. Obviously, two broad absorption bands can be seen from the reflection spectrum of Eu<sup>3+</sup>-doped CaO (Fig. 5a). The maximum at about 248 nm in diffuse reflective spectra are due to the oxygen-to-europium charge transfer band and the weak peak at 345 nm is assigned to typical *f-f* transitions of Eu<sup>3+</sup>. The important observation is that there is not absorption band in the range of long wavelength, which indicates that Eu<sup>3+</sup> was totally incorporated into the CaO lattice and that no new compounds formed. The reason is similar to that case occurred in Pb<sup>2+</sup>-doped SrCO<sub>3</sub>, BaCO<sub>3</sub> and CaCO<sub>3</sub>, which is reported by other scientists [11, 12], and they attributed these phenomena to the adsorption of Pb<sup>2+</sup> ions which had not been built into the carbonate lattice.

FT-IR spectrum analysis

Figure 6a and b shows the FT-IR spectra of the precursor and the sample CaO: Eu<sup>3+</sup> calcined at 1100 °C, respectively. For the precursor, Fig. 6a gave the bands at ~3424, 1420, 1081, 875, and 744 cm<sup>-1</sup>, which could be attributed to OH stretching vibration in adsorbing water, *v*<sub>3</sub> (asymmetric CO stretching) mode, *v*<sub>1</sub> (symmetric CO stretching) mode, *v*<sub>2</sub> (CO<sub>3</sub> out-of-plane deformation) mode and *v*<sub>4</sub> (OCO bending in-plane deformation) mode vibrations of vaterite, respectively. These results suggested that the precursor was vaterite carbonate. In other words, trivalent europium ions and calcium ions were co-precipitated in the form of carbonate. So according to the reaction equation in Scheme 1, the precursor must be calcined.

In order to understand the purity and the internal structure of sample better, the sample was characterized by the FT-IR spectra (shown in Fig. 6b). The characteristic

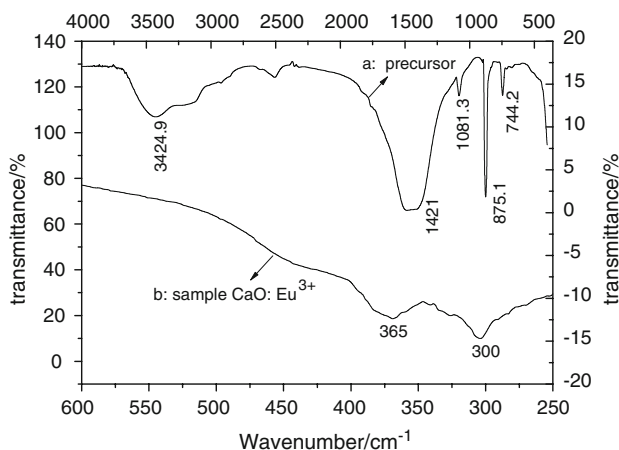


Fig. 6 FT-IR spectra of the precursor (a) and sample CaO: Eu<sup>3+</sup> (b)

absorption bands of carbonate disappear, and the strong peak near 300 cm<sup>-1</sup> is associated with the characteristic absorption of the CaO [13], indicating that CaO: Eu<sup>3+</sup>, which is in good agreement with that of XRD patterns, has been formed calcined at 1100 °C.

Excitation spectrum emission spectrum

Figure 7 shows the excitation spectrum of CaO: Eu<sup>3+</sup> by co-precipitation method. The excitation spectrum was obtained by monitoring at 592 nm radiated from the <sup>5</sup>D<sub>0</sub> → <sup>7</sup>F<sub>2</sub> transitions of Eu<sup>3+</sup>. It can be seen clearly that the excitation spectrum consists of a broad intense band at around 250 nm and is attributed to the charge transfer state (CTS), which are in good agreement with Fig. 5.

The room-temperature emission spectrum of the sample is shown in Fig. 8. The emission spectrum was obtained by monitoring at 250 nm under an excitation of ultraviolet light. The obtained product emitted the red luminescence, which showed the activator Eu<sup>3+</sup> has successfully entered

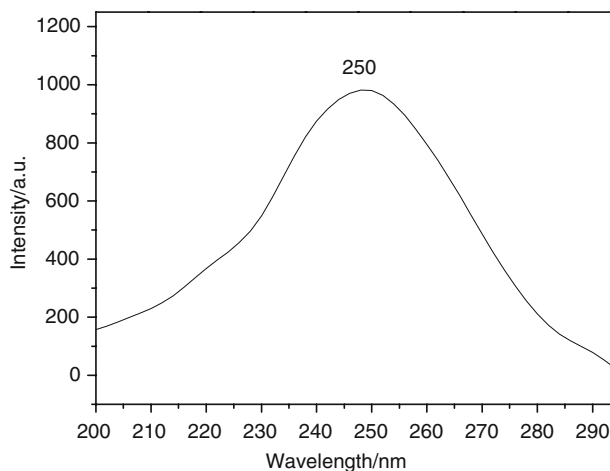


Fig. 7 Excitation spectrum of CaO: Eu<sup>3+</sup>

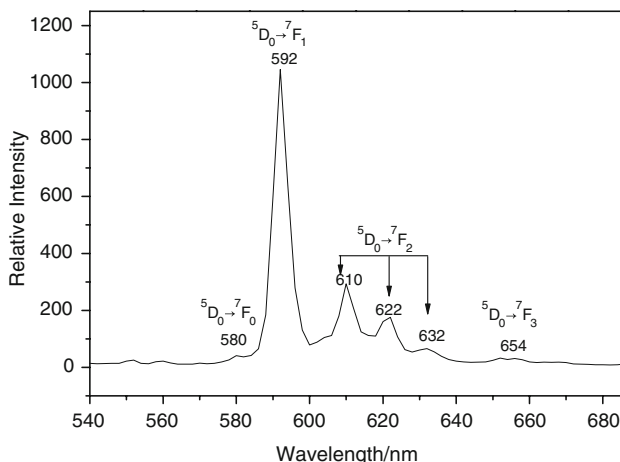


Fig. 8 Emission spectrum of CaO: Eu<sup>3+</sup>

the host lattice of CaO. The characteristic emissions of  $\text{Eu}^{3+}$  were clearly observed including the strongest emission peaks at 592 nm for  ${}^5\text{D}_0 \rightarrow {}^7\text{F}_1$  transitions, 580 nm for  ${}^5\text{D}_0 \rightarrow {}^7\text{F}_1$ , 654 nm for  ${}^5\text{D}_0 \rightarrow {}^7\text{F}_3$  and 610, 622, and 632 nm for  ${}^5\text{D}_0 \rightarrow {}^7\text{F}_2$  transitions. The  ${}^5\text{D}_0 \rightarrow {}^7\text{F}_1$  transition is well known to be mainly a magnetic dipole transition when the  $\text{Eu}^{3+}$  ions locate in a high symmetric position while the  ${}^5\text{D}_0 \rightarrow {}^7\text{F}_{2,4}$  transitions are essentially electric dipole transitions which appears dominantly only when  $\text{Eu}^{3+}$  ion locates at sites without inversion symmetry [14, 15]. Also, from XRD analysis, the sample has the face-centered cubic NaCl structure, which shows that the  $\text{Eu}^{3+}$  ions, occupying the  $\text{Ca}^{2+}$  sites in the CaO lattice, are in sites with high symmetric position ( $\text{O}_h$ ). Furthermore, we note that this line of  ${}^5\text{D}_0 \rightarrow {}^7\text{F}_1$  is not split as is to be expected for symmetry group  $\text{O}_h$ . In these sites, electric dipole transition, such as  ${}^5\text{D}_0 \rightarrow {}^7\text{F}_2$ , is forbidden [16]. Because of selection rule, if  $\text{Eu}^{3+}$  ion locates in symmetric position, optical transitions between the  $4f^n$  configurations are strictly forbidden. However, due to lattice vibration of the host lattice, reducing the symmetry of  $\text{Eu}^{3+}$ , the  ${}^5\text{D}_0 \rightarrow {}^7\text{F}_2$  transition can be observed due to the breakdown of the selection rule. At the same time, the  $\text{Eu}^{3+}$  site must have one symmetric because of no splitting of the  ${}^5\text{D}_0 \rightarrow {}^7\text{F}_0$  transition in the fluorescence spectrum. The fact confirms that  $\text{Eu}^{3+}$  ions mainly locate in strict symmetric position ( $\text{O}_h$ ) of the crystal lattice and the sample belongs to red luminescence.

#### Raman crystal field transitions

The behavior about the Raman crystal field transitions of the rare earth ions in single crystals can be studied by Raman spectrum. This is because the transition between two electronic levels is allowed, if the direct product of their representations contains some of the irreducible representations of the Raman-active phonons [17]. It is highly probable that the observed lines are due to the photoluminescence of  $\text{Eu}^{3+}$  under excitation at 514.5 nm (above the  ${}^5\text{D}_1$  level, at about  $19000 \text{ cm}^{-1}$ ). Moreover, according to Fig. 8, the level of the  ${}^5\text{D}_0$  is 580 nm ( $17241 \text{ cm}^{-1}$ ). So in this paper, all possible intra- and intermultiplets  ${}^7\text{F}_J$  transitions are Raman allowed, such as  ${}^7\text{F}_0 \rightarrow {}^7\text{F}_J$  ( $J = 1, 2, 3, 4$ ) transitions, as shown in Fig. 9.

As can be seen in Figs. 8 and 9, not only has the strongest transition of the  ${}^5\text{D}_0 \rightarrow {}^7\text{F}_1$  one line in luminescence, but also the  ${}^7\text{F}_0 \rightarrow {}^7\text{F}_1$  transition has one line in the Raman crystal field transitions (which is like absorption processes). At the same time, from XRD, the  $\text{CaO}:\text{Eu}^{3+}$  crystals belong to face-centered cubic crystalline  $F_{m-3m}$  and  $\text{Eu}^{3+}$  ions are substituted for the  $\text{Ca}^{2+}$  with  $\text{O}_h$  symmetry. As a result, this will lead to the  $J = 2$  level of  $\text{Eu}^{3+}$  splitting into five or four levels in Raman spectrum, which are in agreement with Fig. 9.

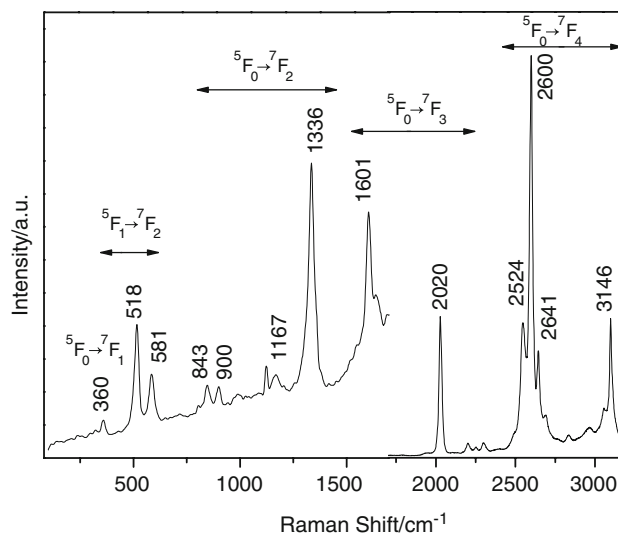


**Fig. 9** Raman spectrum of the sample  $\text{CaO}:\text{Eu}^{3+}$

#### Conclusions

In this work,  $\text{CaO}$  doped with  $\text{Eu}^{3+}$  was synthesized by the co-precipitation method. XRD, laser particle size analyzer, SEM, UV-Vis, FT-IR, PL-PLE and Raman analyses indicated that  $\text{CaO}:\text{Eu}^{3+}$  exhibited a single crystalline structure with many desirable characteristics, such as good morphology, optimum size, high absorption in the UV light range and red luminescence. Thus, this fundamental work may be important in developing new luminescent devices applicable for tricolor lamps, light emitting diodes (LEDs), and so on.

#### References

- Joly AG, Chen W, Zhang J, Wang S (2007) *J Lumin* 126:491
- Conga Y, Lia B, Leia B, Wanga X, Liua C, Liua J, Li W (2008) *J Lumin* 128:105
- Xiao X, Yan BJ (2007) *Mater Lett* 61:1649
- Jeong JH, Yang HK, Shim KS (2007) *Appl Surf Sci* 253:8273
- Fu J (2000) *J Electron Solid-State Lett* 3:350
- Park I, Kima Y, Lee DJ (2007) *J Mater Chem Phys* 106:149
- Di W, Zhao X, Lu S (2007) *J Solid State Chem* 180:2478
- Uhlich D, Huppertz P, Wiechert DU, Justel T (2007) *J Opt Mater* 29:1505
- Liu G, Hong G, Wang J, Dong X (2007) *J Alloys Compd* 432:200
- Zhang H, Lü M, Xiu Z, Wang S (2007) *J Mater Res Bull* 42:1145
- Pan Y, Wu M, Su Q (2003) *J Mater Res Bull* 38:1537
- Lammers MJJ, Blasse G, Brixner LH (1986) *J Mater Res Bull* 21:529
- Srivastava SP, Singh RD (1971) *J Phys Soc Jpn* 31:615
- Ningthoujam RS, Sudarsan V, Kulshreshtha SK (2007) *J Lumin* 127:747
- Gao XR, Lei LX, Lv CG, Sun YM, Zheng HG, Cui YP (2008) *J Solid State Chem* 181:1776
- Liu X, Wang X (2007) *Opt Mater* 30:626
- Taboada S, Andrés de A, Sáez-Puche R (1998) *J Alloys Compd* 275–277:279